Near-Field Characteristics of a Turbulent Coflowing Jet

P.G. Gladnick,* A.C. Enotiadis,† J.C. LaRue,‡ and G.S. Samuelsen§
University of California, Irvine, Irvine, California

The near-field evolution of the velocity and concentration fields for an axisymmetric jet flow of CFC-12 issuing into a coannular jet flow of air is presented. Results based on measurements of the time resolved velocity (two components) and (separately) the concentration, obtained using laser anemometry and Rayleigh scattering systems, show that the transport of momentum and mass in the near field depends on the large scale structure which forms in the shear layer at the edge of the jet. The type of instability and hence the flow development is shown to depend primarily on the ratio of the coflow to jet velocity (m), density ratio, and the jet exit velocity profile. Specifically, for velocity ratios less than and greater than unity, the statistical properties of the velocity and concentration fields are compatible with the existence of an annular vortex ring with positive vorticity for $m<1$ and negative vorticity for $m>1$. For a velocity ratio equal to unity, the results are consistent with the presence of pairs of counter-rotating vortices that are typical of a wake flow.

Introduction

An assessment of combustor performance relative to pollutant formation and overall efficiency requires a careful understanding of the mechanisms of mixing and entrainment in highly turbulent, reacting flows. Reacting flows in practical combustion systems are extremely complex and normally involve turbulent mixing of fuel and oxidizer with recirculation and swirl. The further complication of variable density is created as a consequence of heat release due to reaction.

One approach is to begin with a comparatively simple flow and add complexities to the flowfield in a stepwise fashion. Therefore, one of the initial steps would be to study the effects of central jet to surrounding air velocity ratio and density effects without the inherent complications of chemical reaction, recirculation, or swirl on entrainment and turbulent mixing. An appropriate flowfield is an axisymmetric jet in either a coflowing stream or a coannular jet. The primary interest is in the developing or near-field region of the jet since this is the location in which most of the mixing and reaction would take place.

In the present study, the near field of a jet of CFC-12 (from the jet exit plane to about 15 diameters downstream) in a coflowing air stream and in a coannular jet is studied. The ratio of the jet to coflow gas density is about 3.8, and the ratio of the bulk mean axial velocity in the coflowing air stream or at the exit plane of the coannular jet to that at the central jet exit plane is varied from 0.26 to 2. This corresponds to a variation in bulk, mean, axial, coannular velocity between 0.65 m/s and 4.93 m/s. The central, jet-exit Reynolds number is held constant at about 16,000 (2.43 m/s). Visualization of the flowfields indicates that the coflow velocities are all sufficiently high to prevent fountain effects or recirculation. In addition, centerline, mean-axial velocity decay is measured in freejets of CFC-12, air, and helium in order to compare decay behavior with the work of other investigators and to identify differences in downstream development due to density differences and exit velocity profile. The freejet is chosen for this aspect of the study due to availability of data at a variety of conditions.

The ultimate goal of the research is to acquire an understanding of the flowfield characteristics produced from both recirculation and swirl in a combusting environment. Consequently, nonintrusive instrumentation using laser anemometry and laser Rayleigh light scattering techniques have been developed and are used.

The next section presents a review of related experimental work. In the succeeding section, details of the test conditions, facility, instrumentation, and signal processing are presented. This is followed by one in which the results are presented and discussed with the final section containing conclusions.

Background

Axisymmetric, homogeneous, turbulent jets in a coflowing stream at various ratios of the coflow to jet velocity and in a quiescent ambient have been widely studied with a majority of the emphasis on the far field. Comprehensive reviews are presented by Abramovich[1] and Harsha.[2] More recently, studies of the near-field mixing processes for these types of flow as well as those which include variable density effects have been presented by Durao and Whitelaw,[3] Antonia and Bilger,[4] Shuen et al.,[5] Green and Whitelaw,[6] Pitts,[7] Mostafa et al.,[8] Antonia and Bilger,[11] as well as others. Some investigations, including that of Durao and Whitelaw,[3] have been concerned with the near-field mixing processes of homogeneous, coflowing jets. Those of Shuen et al.[5] and Mostafa et al.[8] have emphasized the impact of a second phase introduced into coflowing jets. Green and Whitelaw[6] and Pitts[7] have concentrated on large-density differences in turbulent jets but have studied primarily free-jets issuing into a still ambient or slow coflow. A more complete review of previous results than that presented here may be found in Gouldin et al.[9] The present work extends the results of these previous studies to a detailed, examination of the relation of large-scale structures in the near field to the mixing processes for a flow consisting of a heavy, central jet and a significantly lighter, coflowing jet with velocity ratios less than, equal to, and greater than unity.

The near field of a jet in a coflowing stream is strongly affected by large-scale structures, which form in the annular shear layer between the two flows as a result of an instability mechanism. The type of instability depends in part on the magnitude and sign of the difference between the coannular and central jet velocity and on the characteristics of the flow at the exit plane and can be characterized by the ratio of the average coannular to central-jet velocity (m). For $m<1$, the instability mechanism has been discussed by Yule[10] and

Received April 5, 1989; revision received Aug. 16, 1989.

†Research Assistant, Department of Mechanical Engineering, UCI Combustion Laboratory.

‡Research Assistant, UCI Combustion Laboratory; currently at Imperial College, London, England, UK.

*Associate Professor, Department of Mechanical Engineering, UCI Combustion Laboratory. Member AIAA.

§Professor, Department of Mechanical Engineering, UCI Combustion Laboratory. Member AIAA.

Michalke[12] and exhibited in the studies of Crow and Champagne,[13] Chen and Roquemore,[14] and Roquemore et al.[15] The shear instability for a velocity ratio less than unity ($m<1$) is that of an annular mixing layer and corresponds to vortex rings, which interact (pair and amalgamate) and in turn undergo an instability process, which leads finally to the fully developed turbulence in the far field. For $m>1$, the flowfield near the jet exit plane at the interface between central and annular jet flow remains an annular mixing layer. A significant difference is that the sign of the mean-velocity gradient for $m>1$ is opposite to that for $m<1$. Thus, for $m>1$, it seems reasonable to hypothesize that the large-scale structures which occur due to the shear instability in the annular mixing layer will be that of a ring vortex but with a sense of rotation opposite to that for $m<1$. At $m=1$, the instability mode *is not* that of an annular mixing layer but rather that of a wake flow, which has its genesis in the boundary layers on the interior and exterior surfaces of the central jet tube. (The instability modes for $m>1$ and $m=1$ have not been observed in previous studies but will be shown subsequently to be consistent with results presented herein.)

The turbulent entrainment and mixing also depends on the jet-exit velocity profile, and the jet-density relative to the ambient. This dependency is due to the corresponding variation of the initial instability mode and resulting large-scale structure, which controls the entrainment and mixing. Thus, the exit conditions are well documented.

This paper complements concentration measurements, previously obtained using laser Rayleigh techniques by Enotiadis et al.,[16] with statistical properties of the velocity field obtained by two-component laser anemometry and spectral properties of concentration using laser Rayleigh scattering. The combined set is analyzed to assess consistency between the two data sets and to develop further insights into the mixing processes in the near field of a turbulent, coannular, heavy jet of CFC-12 exhausting into air for three values of m.

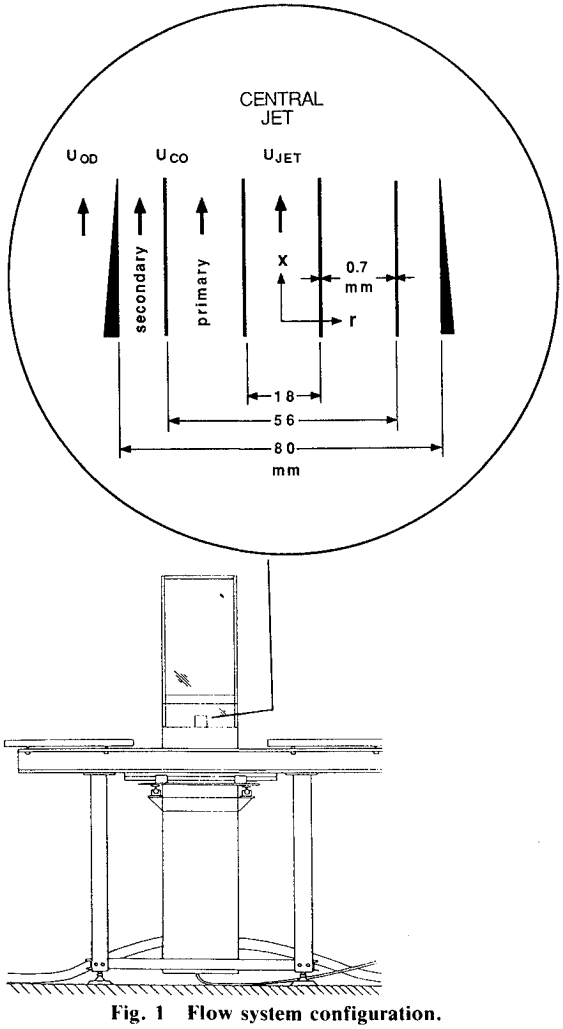

Fig. 1 Flow system configuration.

Experimental Systems

This section contains a discussion of the flow, laser anemometry, laser Rayleigh, and data processing systems.

Flow System

The flow system consists of a 0.7-mm-thick tube for the central jet flow, which has an inside diameter d of 18 mm and is 102 cm in length. The jet tube is surrounded by two concentric tubes. The primary annulus is 56 mm in diameter, and the secondary annulus is 80 mm in diameter. Both tubes are 100 cm in length (see Fig. 1). The middle tube has a wall thickness of 0.7 mm, and the outer tube wall is tapered at 7 deg over the final 110 mm to a knife edge at the exit with a thickness of 0.1 mm. The coannular air stream passes through the annuli formed by these two tubes, and all are equipped with plastic honeycomb 1 m upstream to remove any swirl effects. The secondary (outer) annulus will be used in future experiments. However, since all of the measurements in the present study are in the near field, the existence of the flow in the secondary annulus is assumed to have a negligible effect on the interior flows.

The jet and coannular tubes are mounted on a three-dimensional traverse, which has a resolution of 0.5 mm for concentration data and 0.01 mm for velocity data in all three directions. The entire assembly is orientated such that the jets issue vertically upward. The traverse in turn is mounted to a fixed optical table. All three tubes are centrally located in a square duct, which isolates the flowfield from room air fluctuations. The square duct is 1.5 m long and 457 mm on a side and provides optical access for the laser measurement systems.

CFC-12 is used as the jet fluid, and air is used as the coflow fluid for the parametric study of velocity ratio on mixing. The CFC-12 is supplied to the central jet from four tanks connected in parallel, and the air through the coannular tubes is supplied from a compressor and is filtered by means of mist and particle filters. Both the CFC and air are passed through pressure regulators to maintain constant flow rates which are monitored by rotometers. In addition, the CFC is passed through a temperature bath, which provides a nearly constant temperature (28 ± 2°C) flow. This temperature is high enough to prevent recondensation. For all results reported herein, the bulk jet-exit velocity is held constant at 2.43 m/s. The corresponding Reynolds number is 16,000, which is high enough to insure that the exit velocity profile corresponds to that of a fully developed turbulent pipe flow. This exit profile is chosen as it is easily reproducible and is of fundamental interest.

Free jets of CFC-12, air, and helium are also briefly studied in order to compare mean-axial velocity decay with corresponding results of other investigators and to observe the effects of density differences and exit velocity profiles on the centerline velocity decay. For these mean velocity measurements, the flow facility just described is employed without any coannular air flow. The central jet is supplied from pressurized gas cylinders with the respective gas under study or, in the case of air, from the house supply. Thus, only the central jet is seeded. In the near field, very little unmixed ambient air is found on the centerline. Thus, the lack of seeding in the ambient should have a negligible velocity bias effect on measurements at the centerline. This is supported by the good agreement with the corresponding results of Shuen et al.[5] where both the jet and ambient flows are seeded.

The air flow in the square duct for all experiments is maintained by means of a suction-type system connected to the outlet of the duct, which draws room air through an automotive foam filter. The velocity of the duct air is monitored by means of a calibrated venturi and maintained at a nominal constant value of 0.65 m/s. Visualization of all flowfields

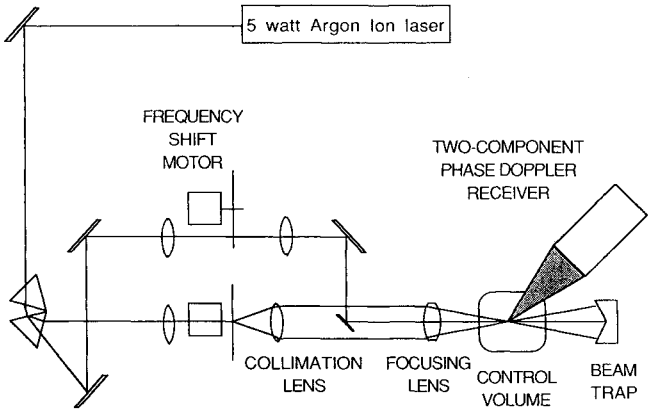

Fig. 2 Laser anemometer system.

shows that this duct velocity is sufficiently high to prevent fountain effects or recirculation inside the duct.

Laser Anemometer

The velocity system used in these measurements is the Aerometrics (model 2100-3), two-component, Phase-Doppler Particle Analyzer (PDPA) operated in the velocity mode for signal collection. Beam transmission is effected by breadboard optics. Figure 2 shows the optical layout employed for the velocity measurements.

The composite laser beam from a 5 W argon-ion laser is split using a prism and spatially separated into two colors centered at 488 and 514.5 nm. In order to distinguish flow directions, frequency shifting of each velocity component by about 1 MHz is implemented with rotating diffraction gratings. Each beam is focused onto its respective diffraction grating. The resultant first-order pairs are then collimated and refocused to form overlapping sampling volumes with orthogonal fringes in the test section. The axial and radial components of velocity are obtained using the receiver of the PDPA. A slit having dimensions of 100 μm (horizontal) by 1000 μm (vertical) is used at the receiver and defines the sample volume length and compensates for any beam wander, respectively. Simultaneity of each component is assessed by collecting data pairs when the percentage overlap of one burst onto the other channel exceeds 1%. Typically, 2000 data samples are sufficient to insure statistical convergence of the mean and rms velocty and shear stress. For example, variations in mean velocity of 0.5%, rms velocity of about 1%, and shear stress of about 1.5% are typical with 2000 samples. A minimum of 5000 velocity samples are collected at each position; although the majority have 10,000 samples associated with each data point. The data rate on average is about 300 samples/s. Data are saved and processed using an IBM AT and the two-component, data acquisition software and processing routines developed by Aerometrics.

Laser anemometry seeding is accomplished with fluidized bed seeding using nominally 1 μm Al_2O_3 particles. The particle density is nearly equal in the central and coannular jets. A new type of seed, which has been mixed with a surfactant serving to discourage agglomeration of particles, is used. This new seed (Micro Abrasives, Inc.) has performed in a manner far superior to that of the common seed material previously used and provides reasonably steady data rates throughout an entire period ($\approx$2 h) of data acquisition.

Laser Rayleigh and Data Processing Systems

The laser Rayleigh system is shown in Fig. 3 and is generally similar to that used by Schefer and Dibble[17] and Pitts[7] except that the composite beam of a 5-W argon-ion laser is used. The laser power supply is equipped with a linear pass-bank filter, which results in a combined noise (including shot noise) and drift of less than 1% in concentration in air. At higher concentrations, the relative noise will be less. The beam is expanded by a factor of 4 and is focused to form a sampling volume with a waist of 35 μm. The Rayleigh scattered light is collected by an f/3.66 achromat lens system and focused onto a 100 by 1000 μm slit, thus, providing a sampling volume of 35 by 100 μm in spatial extent. The time constant for the system is estimated by means of a lumped parameter model where the filtering effect is taken to be of the resistance-capacitance (RC) type. For the photomultiplier used in the present study (Thorn-EMI 9813B), the capacitance of the last dynode is stated by the manufacturer (Thorn-EMI[25]) to be 10 pico farads (pf), and the capacitance of the cable between the output of the photomultiplier and the 1 MΩ termination resistor is determined to be about 45 pf. The corresponding time constant and frequency response (3 dB point) are 55 μs and 2.9 kHz, respectively. The finite time constant leads to an equivalent spatial averaging in the downstream direction, at the maximum mean-bulk velocity of 4.9 m/s, of about 271 μm. Thus, the effective sampling volume is about 271 by 100 μm.

The resultant signal is amplified and then digitized at a rate of 10^3 samples/s by means of a Data Translation 2801-A ADC. For statistical information, 15 s or 15,000 digital samples at each position are processed using a Zenith Z-200 computer using software developed specifically for this purpose.

For power spectra, the signal is low-pass filtered at 2 kHz, and the sample rate is increased to 4 kHz. Fourteen records each of 16,384 samples are digitized. This corresponds to 57 s of data and 229,376 digital samples. The data are immediately stored on floppy disk and subsequently processed using separate Fortran 77 routines, which implement a fast Fourier transform (FFT) algorithm (Microway Inc.) to average all records and to form the average power spectrum. Only records without evidence of particles are used in the computation.

Results and Discussion

The discussion of results is divided into two major subsections. The first deals with the characteristics of the velocity field, and the second deals with those of the concentration field.

Velocity Field

The characteristics of the velocity field at the exit plane are discussed first. This is followed by a discussion of the centerline mean-velocity decay for freejets. Next, results are presented for the jet in a coannular flow.

Exit Plane Conditions

The mixing in the near-field region is substantially affected by the distribution of the velocity field at the exit plane. Confidence in jet symmetry is established by measuring both the axial and radial velocity components across the full jet width 3 mm above the jet-exit plane. Mean velocity values at all corre-

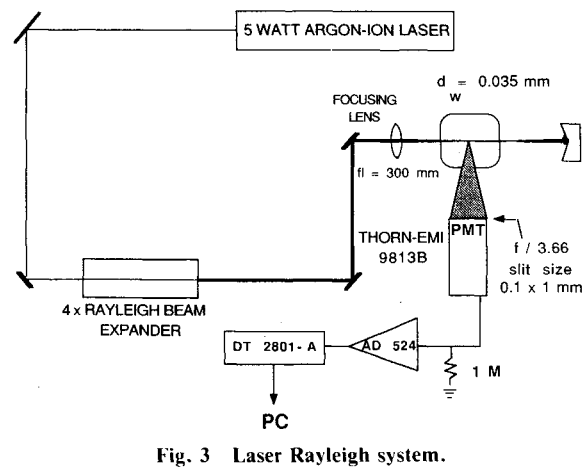

Fig. 3 Laser Rayleigh system.

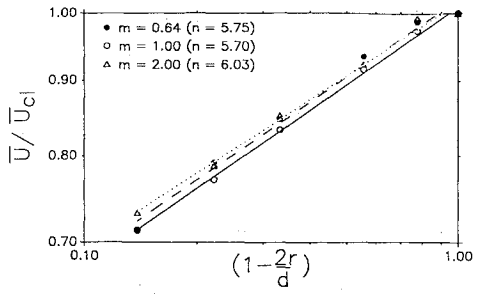

Fig. 4 Central jet power law approximation.

sponding positions on opposite sides of the centerline differ by less than 3% near the tube lips and less than 1% in the central regions. Corresponding spatial pairs in regions of high-velocity gradient possess rms values, which differ by less than 5% near the tube lips and less than 2% at all other locations. Corresponding values of the Reynolds stress agree within 10% over the entire width of the jet.

Exit velocity profiles of the jet will affect the mixing behavior as a result of differences in the magnitude of the velocity gradients near the edge of the jet. Figure 4 shows that the mean velocity profile near the exit of the central jet is well described by a power law, which is consistent with fully developed turbulent pipe flow. For the three velocity ratios investigated, good agreement with the expected value of 6 for the power law exponent (n) is found. The velocity ratio (m) has been defined as the ratio of the bulk velocity in the coannular stream to that in the central jet. Ratios of interest are those corresponding to different mixing behavior, which have representative values less than unity ($m=0.64$), equal to unity ($m=1.00$), and greater than unity ($m=2.00$). For comparative purposes, the corresponding ratios using the maximum mean axial velocity in each stream are, respectively, 0.62, 0.95, and 1.72.

The exit mean and rms axial and radial velocity and shear stress profiles for each velocity ratio are shown separately in Fig. 5. The mean-axial velocity profiles for all velocity ratios correspond to fully developed turbulent pipe flow except that of the secondary annulus flow for $m=0.64$ where the Reynolds number is 2300, and the exit profile is transitional. For all velocity ratios at the exit plane, the location of the tube lips are readily identifiable by associated local minima in axial velocity and sign transition in the radial component, which correspond to wakes from the inner and outer edges of the jet and coannular tubes at r/d of 0.51 and 1.57.

Exit mean-radial velocities exhibit different behavior depending on the velocity ratio. For $m=0.64$, the central jet is seen to have a weak mean radial velocity toward the jet centerline (negative value) near the inner edge of the central jet tube at $r/d=0.5$; whereas over the majority of the central jet area there is a weak positive radial velocity tending to spread the jet away from the centerline. In contrast, for $m=2$, a strong negative radial velocity toward the jet centerline is seen to prevail over the entire jet area, which linearly decreases to zero at the jet center. This is compatible with the view that the annular vortex rings grow toward the jet centerline for velocity ratios greater than unity. For the velocity ratio $m=1$, the radial velocity at the inner edge of the jet tube is seen to have a greater negative magnitude than for $m=0.64$. However, it quickly decreases to zero and remains there over the majority of the jet area. This behavior, coupled with the mean-axial velocity shape above the central jet tube lip at $X/d=3$, indicates that the jet fluid is not spreading or contracting appreciably in the region near the jet exit plane ($X/d<3$).

The velocity profiles measured at the exit plane of the annuli are consistent with the fully developed turbulent annuli measurements of Brighton and Jones.[18] Better agreement for higher velocity ratios is found in contrast to those with low values of the Reynolds numbers. For example, positions of maximum mean-axial velocity are found to occur within 15% of the positions found by Brighton and Jones[18] where transitional Reynolds numbers are involved $Re_{(prim.)}=3700$, $Re_{(s)}=2300$ with $m=0.64$. However, positions of maximum mean-axial velocity are found to occur within 3% of those

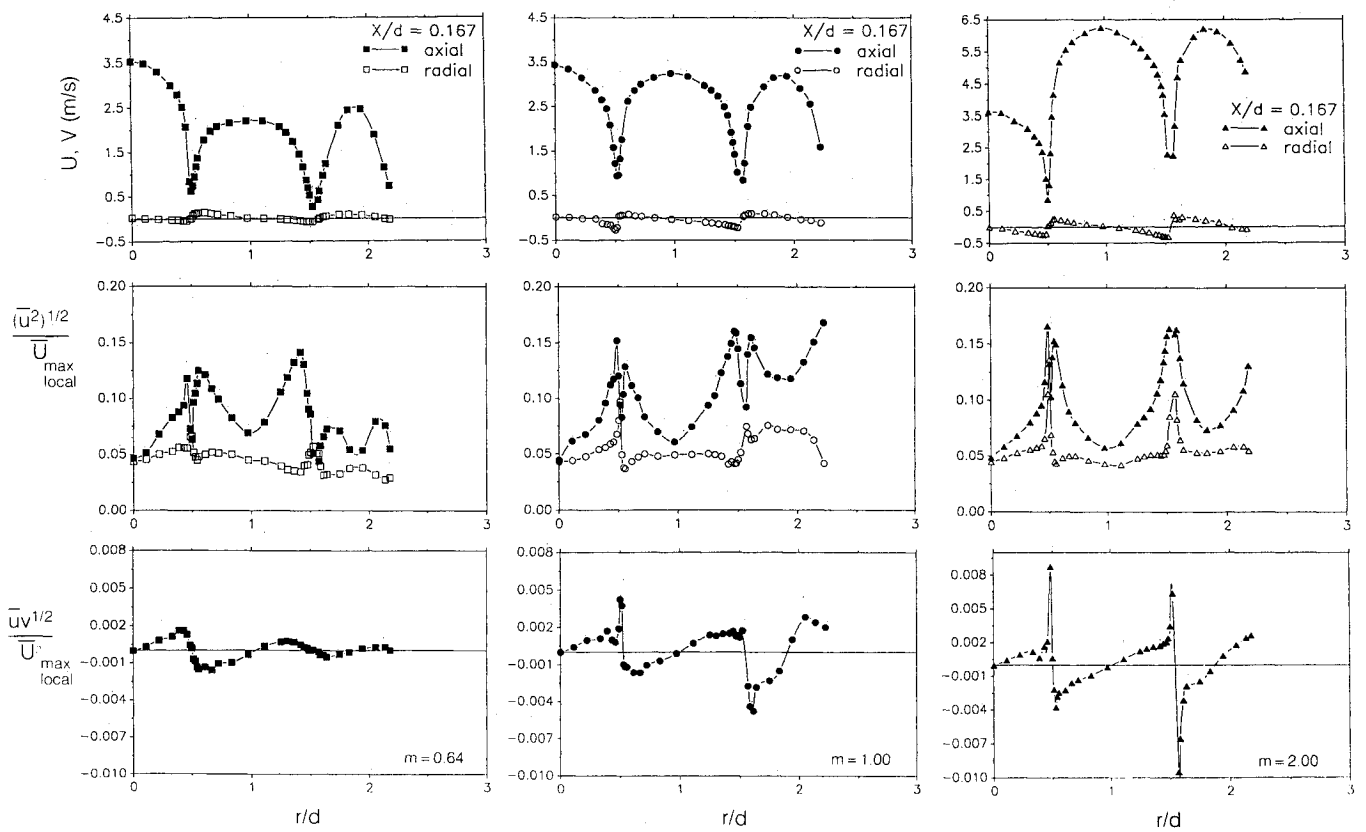

Fig. 5 Exit velocity profiles.

Table 1 Experimental parameters of various coannular and free jets

Reference	d_{jet}(mm)	Re^a	Exit[b] profile	Fluid	Jet type[c]
Shuen et al.[5]	16.00	23,000	FDTPF	Air	F
Green et al.[6]	10.00	16,900	TTHP	CFC-12	F
Mostafa et al.[8]	24.10	5,700	FDTPF	Air	C
Durao and Whitelaw[3]	16.13	27,800	FDTPF	Air	C
Present	18.30	16,000	FDTPF	CFC-12	C/F
		16,000	FDTPF	Air	F
		4,000	FDTPF	Helium	F

[a]Central jet.
[b]FDTPF (fully developed, turbulent pipe flow); TTHP (turbulent, top-hat profile).
[c]F (freejet); C (coannular jet).

found by Brighton and Jones[18] at the higher velocity ratio cases where the Reynolds numbers are high enough that fully developed turbulent flow is expected.

For all velocity ratios, as shown in Fig. 5, the minimum rms axial velocity occurs at the position where the gradient of the mean-axial velocity is zero. At the exit plane, the rms velocities are normalized by the maximum mean-axial velocity in *each* of the three respective streams. The rms axial-velocity increases with increasing radial distance from the zero mean gradient position at the jet centerline. The maximum intensities in each of the three flows occur at radial positions where the mean-velocity gradient is a maximum. For $m=0.64$ and 1, the rms axial velocity decreases as the position corresponding to the midpoint of the tube lip is approached. These relative minima in the rms axial velocity occur downstream of the center of the lips.

The wake regions above the tube lips at the exit plane become progressively thinner with increasing velocity ratio. This is consistent with the reduction of the region of high-velocity gradient near the tube surfaces as the velocity in the annulus is increased. Above the central jet tube lip, the peaks in axial rms velocity for $m=0.64$ are separated by 2 mm. Increasing the velocity ratio to $m=1$ reduces the separation of the peak rms axial velocity to 1.75 mm. A further increase to a velocity ratio of $m=2$ reduces the separation of the peaks to 1 mm. A corresponding reduction in the separation of peaks in the rms axial velocity above the tube lip separating each annular jet also takes place as the velocity ratio is increased. Here the separation between axial rms velocity peaks progressively decreases from 4 to 2.5 to 1 mm. Because of the finite spatial resolution of the measurements taken in this region (250 μm increments), the relative minimum in rms axial velocity at the center of the tube wake is not as noticeable in the profiles corresponding to $m=2$ since the wake is only slightly larger than the separation in radial position where data are collected.

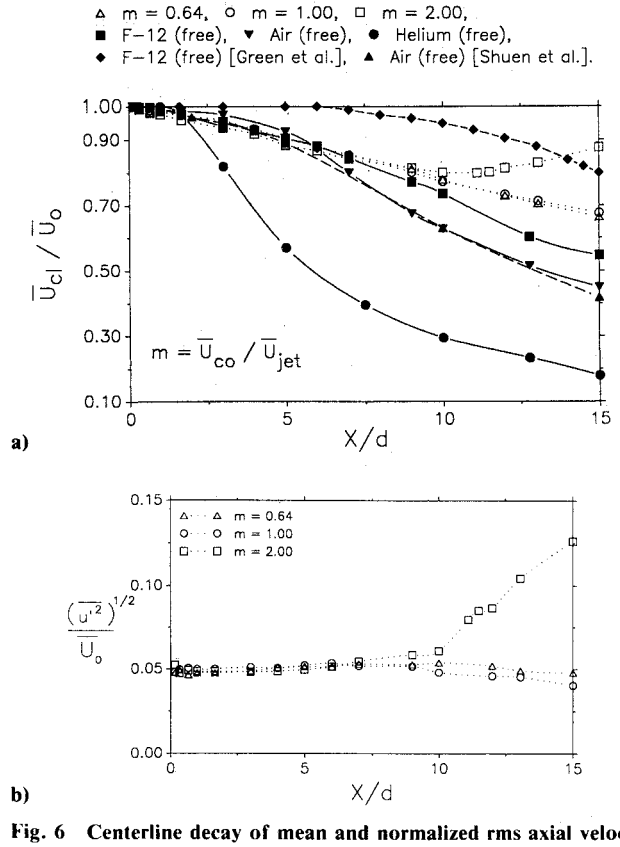

Fig. 6 Centerline decay of mean and normalized rms axial velocity.

The turbulence intensity at the exit of the central CFC jet for this study has a nominal value of 4.5%. In addition, the radial rms velocity becomes nearly equal to the axial rms velocity at the centerline. This is in agreement with the results of Laufer[19] for a turbulent pipe flow. Exiting turbulence intensities from the primary coannular jet at the position of maximum mean axial velocity vary from about 7 to 6.1 to 5.8% as m varies from 0.64, 1, and 2. Therefore, the relative intensity in the primary coannular jet decreases with increasing velocity. In the secondary annular flow, there is no comparable trend in the turbulence intensity. This is likely due to the transitional exiting velocity profile for $m=0.64$, which possesses a relatively low turbulence intensity of 5.4%.

A comparison of shear-stress profiles with the mean-axial velocity profiles at the exit region reveals that the shear stress is zero at locations of zero mean-axial velocity gradient—specifically on the centerline and near the midpoints of each annulus. Abrupt changes in the sign of the mean velocity gradient observed, for example, at $r/d=0.51$ and 1.57, correspond to a change in the sign of the shear stress. It appears that there is a correspondence between the Reynolds stress and the negative of the mean velocity gradient.

Variation of Centerline Velocity

Differences in the centerline decay of the mean axial velocity for a turbulent jet in a coflowing stream are dependent on the shape of the exit velocity profiles and density and velocity differences. The effects of variation of these parameters is evident in the decay data shown in Fig. 6a for various coannular and freejets except in the initial region ($X/d<1.25$) where the results are similar. Here the data are normalized by the centerline axial velocity measurement taken at $X/d=0.167$. Experimental parameters of importance from results compared with the present work are listed in Table 1. Beginning with freejets, the centerline decay of a CFC-12, freejet, which has an exit axial velocity profile which is fully developed (present) in contrast to one where the exit velocity profile has a "top hat" shape[6] behaves differently; even though the Reynolds numbers are about the same (16,000). In the present case, the mean velocity begins to decrease closer to the jet exit. This is due in part to the fact that the jet momentum in the present study is less than that in the flow of Green and Whitelaw[6] as the velocity gradient exists acros the entire radius of the jet instead of only at the edges.

The effect of density on the decay of the centerline, mean, axial velocity for freejets can be seen by comparing the decay of CFC-12 ($Re=16{,}000$), air ($Re=16{,}000$), and helium ($Re=4000$). As expected (compare Corrsin and Uberoi[20] and

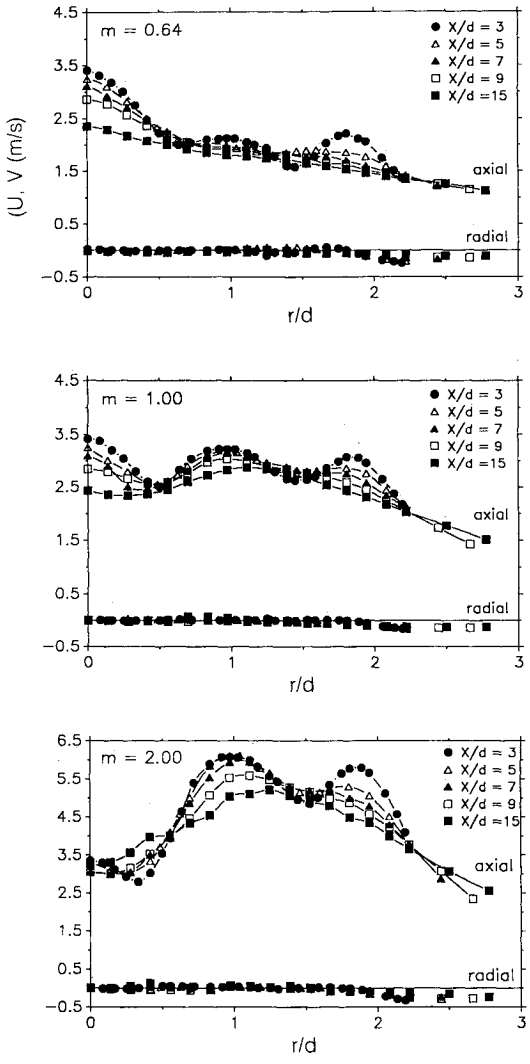

Fig. 7 Development of mean axial and radial velocity.

Thring and Newby[21]), the mean-axial velocity decays faster for the jet with the less dense gas and slower for the jet with the more dense gas. Good agreement with the data of Shuen, et al.[5] is found for the free-air jet.

The addition of a coflowing stream about the CFC jet increases the coflow momentum such that the rate of decay of the centerline, mean-axial velocity is less than that of the free-jet counterpart having the same fluid and turbulent velocity exit profile. Although the decays of mean velocity for $m \leq 1$ are similar, at $m = 2$, a trend reversal occurs in decay at about $X/d = 9$ where, after the initial decrease, the mean velocity begins to increase.This is attributed to momentum transfer from the annular flow to the central jet flow. A similar trend is found by Durao and Whitelaw[3] with coflowing air jets with $m = 1.61$. In their study, the location of reversal occurs at $X/d \sim 6$, which is slightly upstream of the value found in the present study. The higher exit Reynolds numbers, lighter density gases, and thicker-walled jets (2.73 mm) in the study of Durao and Whitelaw[3] contribute to the earlier trend reversal in the mean axial velocity.

The centerline variation of normalized axial rms velocity with downstream distance is shown in Fig. 6b. The trend reversal for the case $m = 2.00$ that exists for the mean-axial velocity is present at the same downstream location in the rms axial velocity. Here the transition away from the centerline decay for the other two velocity ratios begins at about $X/d \approx 7.5$ and increases dramatically at $X/d = 10$. At the axial location of $X/d = 15$, the normalized rms velocity for this velocity ratio ($\approx 13\%$) is roughly three times greater than the other two cases ($\approx 4.5\%$). In this respect, velocity ratios greater than unity are distinguished in that a significant increase in centerline mean velocity is accompanied by a higher fluctuation intensity in the near field.

Radial Variation of Mean, rms, and Shear Stress

The variation of mean and rms axial and radial velocity and shear stress are shown in Figs. 7–9 for all velocity ratios at axial stations for $3 \leq X/d \leq 15$. As shown in Fig. 7, the mean-axial velocity peaks, which mark each individual fluid stream, persist to $X/d = 5$ for $m = 0.64$ and to $X/d \approx 7$ for $m = 1$ and 2.

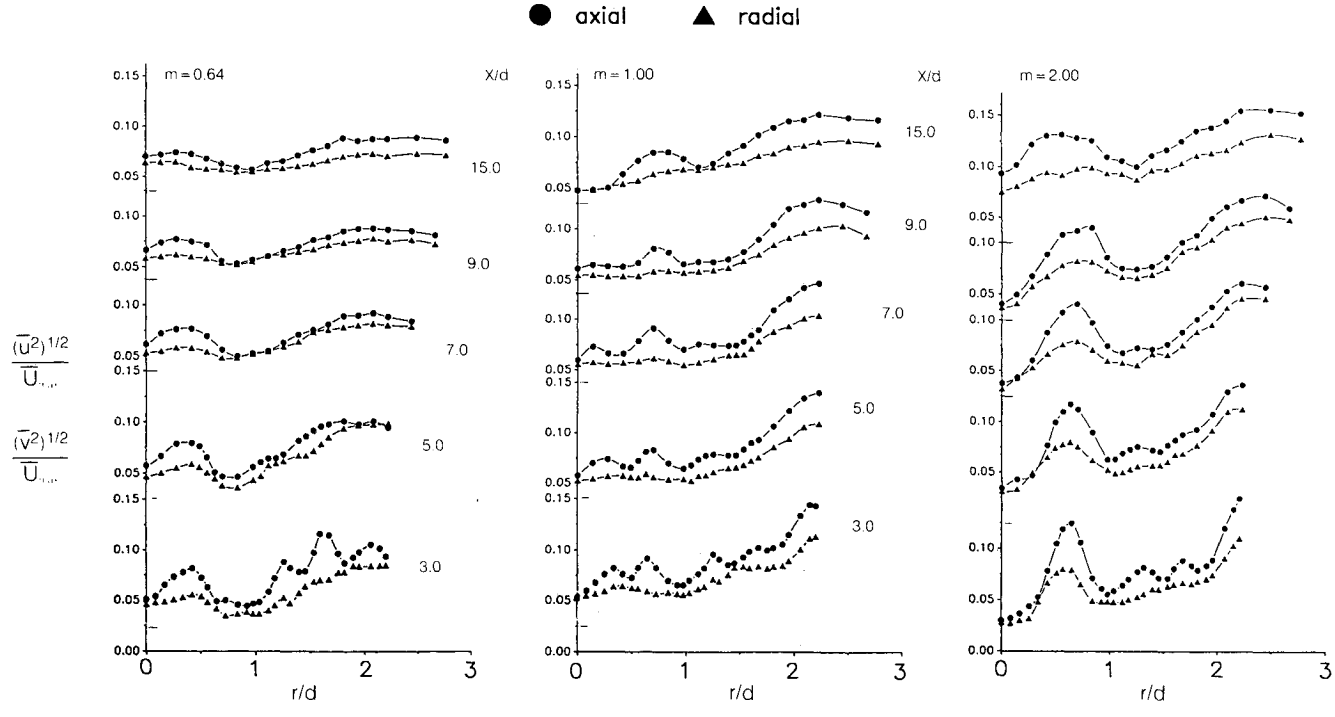

Fig. 8 Development of normalized rms velocity.

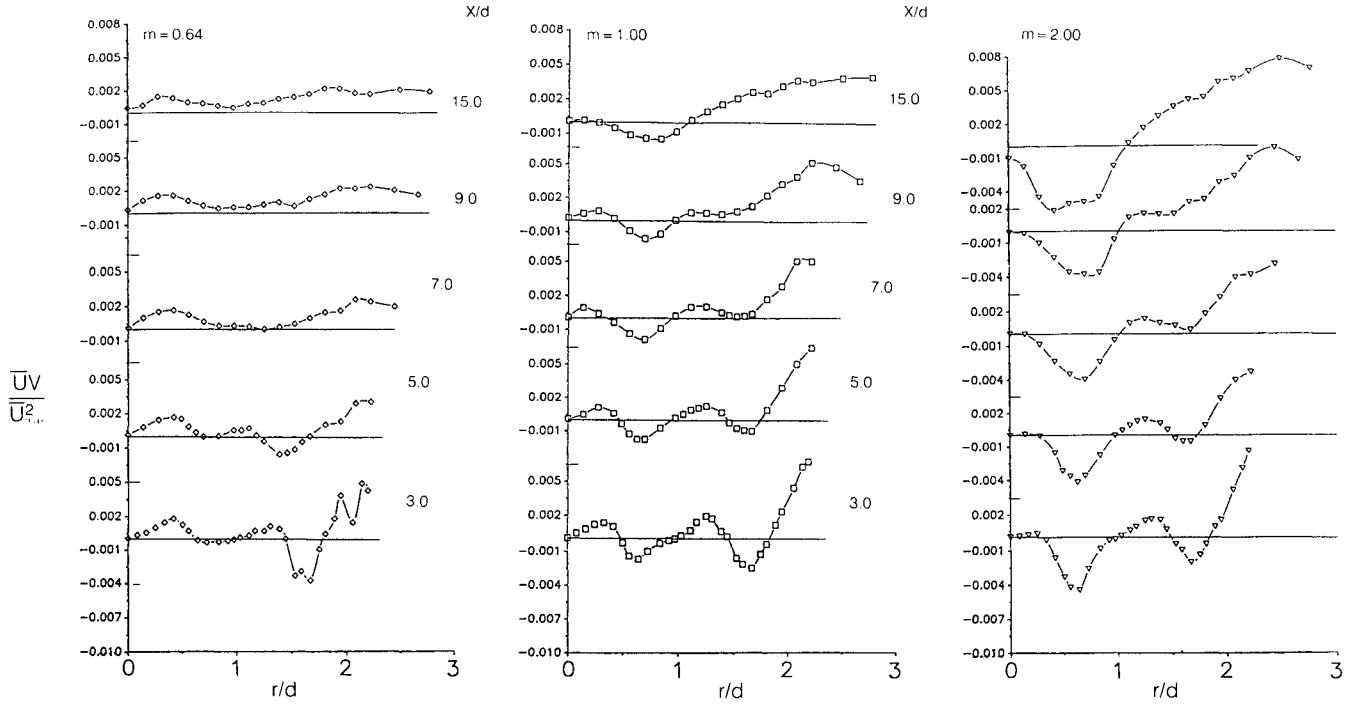

Fig. 9 Development of Reynolds stress.

The mean-radial velocity is essentially constant for $X/d \geq 3$ for all cases, although entrainment of the slow moving duct air is indicated by the negative mean-radial velocity values in the outer region of the secondary coannular jet. The mean-axial and radial-velocity profiles for all velocity ratios investigated indicate that the mean-velocity field is developing over the entire near field ($X/d \leq 15$) and that self-similarity is not reached.

Normal stress profiles presented in Fig. 8 for each velocity ratio exhibit differences which correspond to the three fundamental modes of instability found for velocity ratios less than, equal to, and greater than unity. Here, for each velocity ratio, the rms velocity is normalized by the maximum mean axial velocity of the three streams.

For $m = 0.64$, the outer peaks in the axial and radial rms velocity profiles are significantly reduced in amplitude by $X/d = 5$. This position corresponds to the disappearance of distinct/separate flows in the velocity field and coincides with the lack of local peaks in axial mean velocity at the same location. The innermost peak broadens and is reduced in amplitude with downstream distance.

The development of the rms velocity profiles for $m = 2$ is similar in some respects but different in other respects from that for $m = 0.64$. For example, for both $m = 2$ and 0.64, the inner peaks in the rms-axial and radial-velocity profiles which are observed at $r/d \approx 0.5$ and $X/d = 3$ broaden and are reduced in amplitude with downstream distance. In contrast, with increasing downstream distance, the position of the maxima of the inner peak moves radially *outward* for $m = 2$ but moves radially *inward* for $m = 0.64$. This difference in the direction of the radial movement corresponds to the fact that the sign of the vorticity of the annular vortices at $m = 2$ is opposite to that at $m = 0.64$. For $m = 2$, similar to the development of the rms profiles at $m = 0.64$, the two outer peaks at $r/d \approx 1.25$ and 1.6 and $X/d = 3$ have nearly disappeared by $X/d = 5$.

Noticeable differences between the rms-axial and radial velocity profiles can be seen when comparing corresponding rms velocity profiles of matched velocity streams ($m = 1$) with those for $m = 0.64$ and 2. For example, for $m = 1$, two peaks in the axial rms velocity, in contrast to only one peak, exist on either side of the central tube lip to $X/d = 9$. For $m = 1$, the inner peak diminishes at $X/d \approx 9$, whereas the outer peak remains evident throughout the range of measurements and moves outward. Differences also exist in the radial, rms velocity profiles for $m = 1$ when compared with those of the other two cases. For example, starting at $X/d = 5$ for $m = 1$, the radial rms profile has nearly a constant value for $0 < r/d < 1$ but monotonically increases as the outer edge of the jet is approached. In contrast, for $m = 0.64$ and 2, a relative maximum is noted at $r/d \approx 0.45$. The absence of any such peak at this radial location for $m = 1$ and $X/d > 5$ indicates that, on average, radial transport of coherent structures is minimal. As expected, at radial postions greater than 1.25, the axial and radial rms velocity at $m = 1$ are similar to those at $m = 0.64$ and 2.00.

Downstream of the edge of the central jet-tube wall, the single peak in the rms-axial and radial-velocity profiles coupled to the higher-velocity fluid stream for $m = 0.64$ and $m = 2$ is consistent with the hypothesis that a single annular vortex which dominates the mixing exists in the developing region of these flows. Two peaks in the axial rms velocity profile for $m = 1$ at $r/d \approx 0.5$ are consistent with the existence of pairs of vortices, which is typical of a wake flow.

The variation of Reynolds shear stress with downstream distance for each velocity ratio is presented in Fig. 9. The shear stress is zero at locations of zero mean axial velocity gradient and is proportional to the negative of the radial gradient of the mean axial velocity for all velocity ratios. Since the mean velocity of each coannular stream is nearly equal for each velocity ratio, the shape of the shear stress profiles in the annuli ($r/d \geq 1.25$) are similar for all m. However, the magnitudes of the shear stress increase with increasing mean axial velocity.

The sign of the local peaks in shear stress at $r/d \approx 0.5$ indicates a fundamental difference in the annular vortex for the flows with $m = 0.64$ and 2. The positive local peak in shear stress for $m = 0.64$ corresponds to a positive axial-positive radial velocity correlation, which would correspond to an annular vortex with positive vorticity. In contrast, the negative local peak in shear stress for $m = 2$ corresponds to a positive axial-negative radial velocity correlation, which would correspond to an annular vortex with negative vorticity. These correlations coupled with the fact that the peak moves inward for $m = 0.64$ and outward for $m = 2$ agrees with the hypothesis that the annular vortices have opposite sign and play a significant role in the mixing and entrainment process in the near field. Downstream of the edge of the central jet tube wall for $m = 1$, two local peaks in shear stress are situated to either side

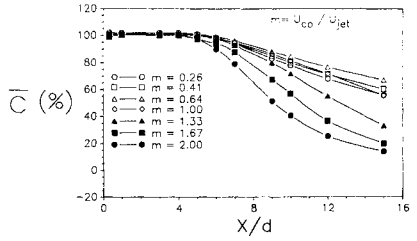

Fig. 10 Centerline variation of mean concentration.

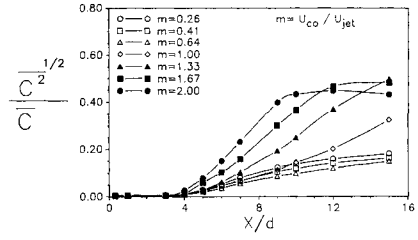

Fig. 11 Centerline variation of normalized rms concentration.

of $r/d = 0.5$, one with a postive and one with a negative velocity correlation. The persistence of these two local peaks throughout the near field to $X/d \approx 9$ gives evidence of the existence of pairs of counter-rotating vortices.

Near-Field Development

The mean-axial velocity profiles do not attain a self-similar shape by $X/d = 15$ since the profiles, except at the low coflow ratio, still contain regions with positive radial gradients. In contrast, the results of Mostafa et al.[8] reach self-similarity by $X/d = 12.5$ for a coflowing air jet of area ratio $A_0/A_i = 0.87$ with velocity ratio $m = 1.40$ where A_0/A_i is the area ratio between the external and internal nozzles. Part of the reason for this difference may be that the wall of the jet of Mostafa et al.[8] is relatively thick (2.45 mm) compared to the wall thickness of 0.7 mm in the present study. In addition, the difference in density ratio between the present study and that of Mostafa et al.[8] is consistent with the finding that the heavier CFC jet decays on centerline at a slower rate than the less dense jets of air or helium. The results of Durao and Whitelaw[3] reach self-similarity at about $X/d \approx 30$ for a coflowing air jet of area ratio $A_0/A_i = 5.79$ with velocity ratio $m = 1.61$. Again, a thick-walled jet of 2.73 mm is used. Nonetheless, these results are consistent with the observations of Champagne and Wygnanski[22] for coflowing turbulent jets with top-hat exit profiles where the length of the central jet core increases with increasing area ratio. Thus, the position where self-similarity is reached in coflowing jets is postponed with increasing area ratio. It is reasonable that this result would apply to coflowing turbulent jets with fully developed velocity exit profiles. For the present study, the ratio of the area of the primary annulus to the area of the central jet is 8.60. This suggests that self-similarity will be reached downstream of $X/d = 30$.

Concentration

Centerline Variation of Mean and rms Concentration

The near-field concentration characteristics of the CFC jet in a coflowing stream also show that the instability mechanism plays an important part in the developing region of the concentration field. Figures 10 and 11 show the axial centerline variation of mean CFC concentration and unmixedness for velocity ratios $0.26 \le m \le 2$. The similarity in the data for $m < 1$ and separately for $m > 1$ is evident in the mean and normalized rms profiles. Comparison of these data with those for the case where $m = 1$ reveals that the development for streams with matched velocities differs from the other two cases.

The similarity of the profiles corresponding to $m < 1$ is clear in both figures, where it can be seen that the rate of decrease of mean concentration with X/d (see Fig. 10) increases with *decreasing* velocity ratio. This behavior is qualitatively similar to that for the decay of mean centerline temperature as a function of m found by Antonia and Bilger[4] for a heated round jet in a coflowing stream. In contrast, for $m > 1$, the rate of decrease of mean concentration increases with *increasing* velocity ratio. This behavior is consistent with the idea that the strength of the annular vortex increases as the relative difference between the CFC jet and coannular air-stream velocities increases and hence leads to more rapid mixing and an increase in the rate of decrease of the mean concentration.

When average mean exit velocities are matched, i.e., where $m = 1$, the centerline decay of mean and rms concentration are seen to differ from the behavior for velocity ratios greater than or less than unity. Although the magnitude of the mean concentration is about the same as those for $m < 1$, the rate of decay is quite different and leads to a decay curve that crosses over the other three mean concentration curves. This suggests a mixing mechanism uniquely related to this particular velocity ratio. The normalized rms concentration is seen to follow a similar trend by crossing over the family of curves for $m < 1$ before increasing further downstream (see Fig. 11).

Radial Variation of Mean and rms

The radial variation of the mean concentration for velocity ratios of 0.64, 1, and 2 at axial locations between $X/d = 0.33$ and 15.0 are shown in Fig. 12. In contrast to the exit-velocity profiles, those of the mean concentration possess a top-hat-like shape. Independent of downstream location, the mean concentration profiles show a nearly common "crossover" point at $r/d \approx 0.53$. The mean value at the crossover point decreases with increasing velocity ratio but the radial location remains almost constant.

The radial variation of rms concentration with axial distance is shown in Fig. 13. For $m = 0.64$, the peak in rms con-

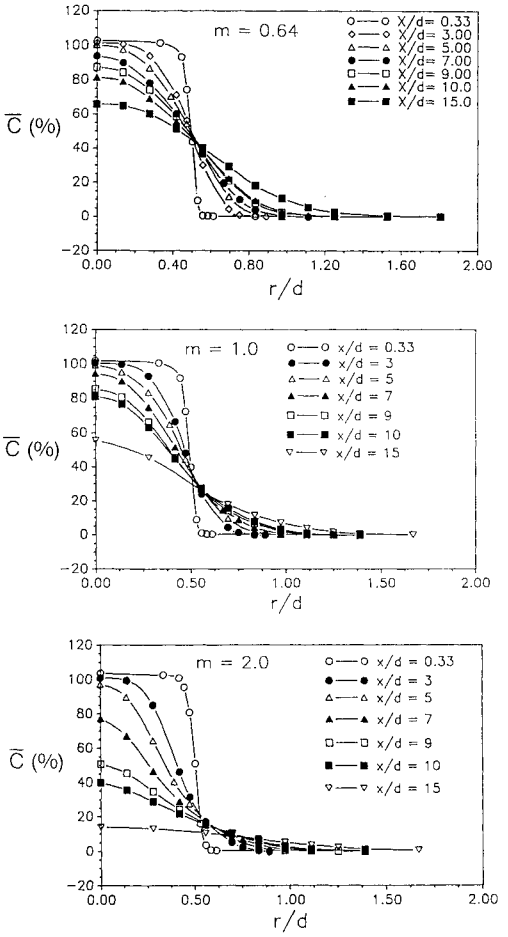

Fig. 12 Radial variation of mean concentration.

centration moves slightly away from the central jet axis with downstream distance and maintains a local minima on the jet axis throughout the measurement range. For $m=1$, a slight shift in the peak rms concentration toward the jet axis occurs with downstream distance and its local minima remains on the jet centerline. When the velocity ratio is further increased to $m=2$, deviation from the other two velocity ratio cases occurs. A local minimum in rms is found on the centerline as far as $X/d=7$ after which the jet axis becomes the location of the maximum concentration fluctuation. The peak in rms concentration, which originates in the shear layer between the CFC and air streams, has now traveled onto the jet axis. This is consistent with the increased mixing observed in the decay of axial centerline concentration at this velocity ratio.

Power Spectra for Concentration

Power spectra of concentration are measured for velocity ratios of $m=0.26$, 1, and 2. For velocity ratios less than and equal to unity, the power spectra show no significant peaks throughout the measurement range ($0.33 \le X/d \le 15$) on centerline or at the position where $r/d=0.5$. Figure 14 shows the power spectral density function (PSDF) of concentration for $m=2$ at normalized radial locations of 0.0 and 0.5 for various downstream positions. The axial variation of the centerline PSDF shows that, from the exit plane to about $X/d=9$, all of the energy is nearly constant in the range of frequencies from 0.5 to 90 Hz with no relative maxima present on the centerline. However, a small spike appears which grows in amplitude and definition from $X/d=9$ to 15. The corresponding frequency is about 30 Hz. Above the central jet tube lip at $r/d=0.5$, a spike at a frequency of 135 Hz is seen to exist. This peak grows in magnitude and definition and shifts to lower frequencies and broadens at each successive downstream location. By

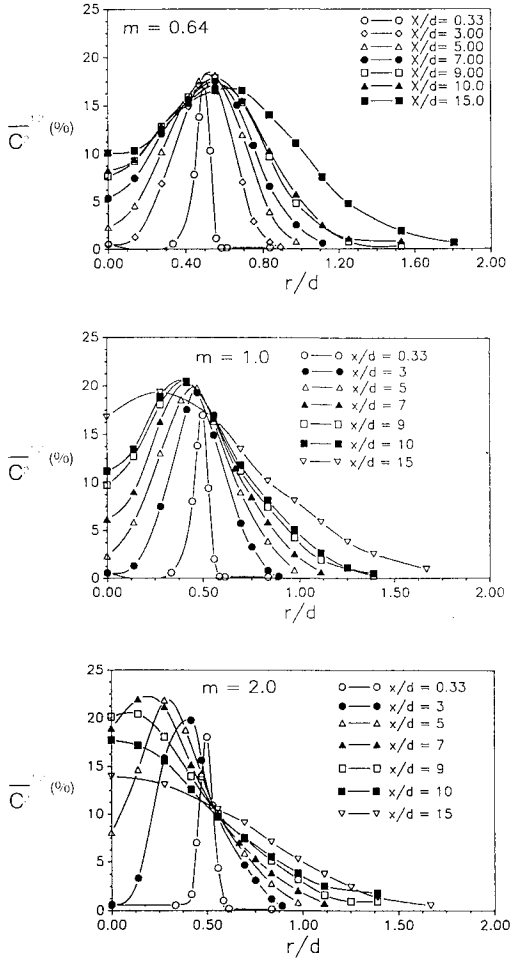

Fig. 13 Radial variation of rms concentration.

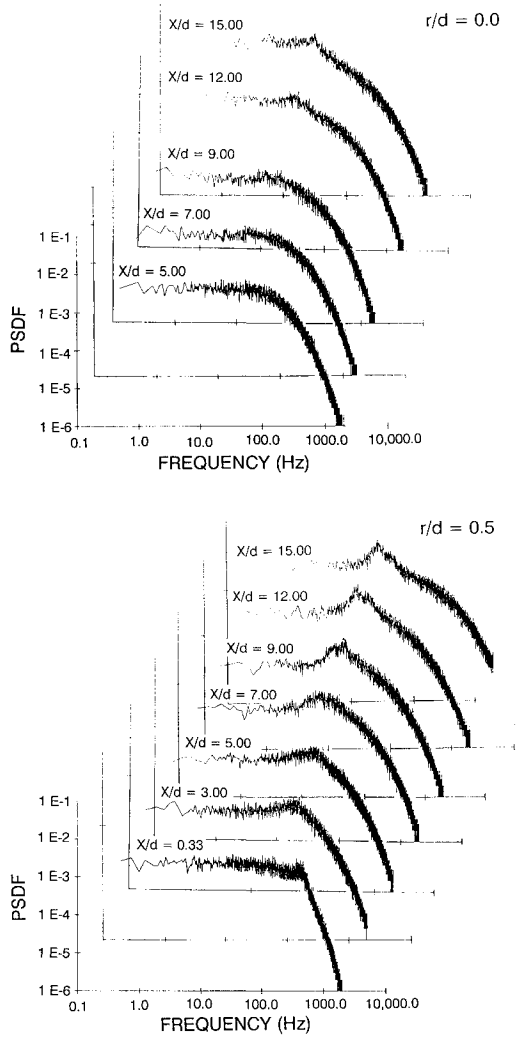

Fig. 14 Power spectral density function of concentration.

$X/d=9$, two peaks in frequency, one at 50 Hz, carried over from the previous axial station ($X/d=7$) and the other at 35 Hz, coexist.

Support for the growth in size of ring vortices whose origins are at the interface between CFC and air streams ($r/d=0.5$) with negative vorticity and growth or movement toward the jet axis is found in the appearance of the 30 Hz frequency spike on centerline *and* at $r/d=0.5$ ($X/d=9$) coupled with the existence of a 50-Hz frequency spike at $r/d=0.5$ ($X/d=7$) with *no* such spike on the centerline. Between the axial stations, $X/d=7$ and 9, the size of the vortices grow sufficiently to indicate their presence on the jet axis at $X/d=9$. An estimate of the vortex length scale at this axial station is the central jet diameter. This axial location also coincides with an increase in mean centerline velocity and relative intensity (see Figs. 6a and 6b) as well as a reduction in the rate of increase of relative concentration intensity (see Fig. 11). Thus, it appears that the presence of the large vortical structures at the centerline have a significant effect on the statistical properties of the velocity and concentration field.

Conclusions

Inlet boundary profiles of velocity and concentration are found to influence the decay of centerline, axial, mean velocity, and mean concentration significantly. A jet with a turbulent, pipe-flow-type, exit velocity profile is found to decay more rapidly than a jet with a top-hat exit profile.

The instability mechanism and resulting large-scale vortical structures are shown to play an integral part in the developing region of an axisymmetric coannular jet. For m less than,

equal to, and greater than unity, there are significant differences in the centerline decay of mean velocity and concentration and an increase of relative concentration and intensity. These differences, along with the relative peak found in the power spectra of concentration for $m=2$ and the previous studies of jets in coflows with $m<1$, support the hypothesis that the near-field mixing of a jet in a coflowing stream is dominated by the large-scale structures which evolve from an instability in the shear layer occurring at the interface between the central and coflow jets. Further, the differences in the change of the statistical properties of the velocity and concentration field with downstream distance strongly supports the hypothesis that depending on whether m is less than, equal to, or greater than unity, different large structures dominate the near-field mixing process. For $m>1$, the results are consistent with the presence of an annular vortex ring with positive vorticity, which has been observed in previous freejet studies. The present results extend those observations and show that for $m>1$, the results are consistent with the presence of an annular vortex ring with negative vorticity. The strength of these vortices increases with increasing velocity difference between the jet and coannular flows. Mixing and entrainment are also found to increase with increasing velocity difference. For $m=1$, the results are consistent with the presence of pairs of counter-rotating vortices which are typical of a wake flow.

Power spectra of concentration on centerline and at the jet radius indicate the presence of periodic structures for $m=2$, which correlate well with the statistical trends of the velocity and concentration fields. The increase in mixing on the jet centerline for velocity ratios greater than unity is found to be the result of central jet penetration by the growth of large scale structures whose genesis is at the shear interface between central and coannular jets. For $m\leq 1$, the vortical structures are apparently not periodic.

Acknowledgments

The authors wish to acknowledge V.G. McDonell for his indispensible expertise, insight, and assistance regarding the phase Doppler and velocity measurements; Howard Crum and Jeff Emdee for their help in the design and construction of the test facility; Erik Alson for help in preparing the final figures; the staff of the UCI Combustion Laboratory; and the National Science Foundation for their continued support under Grant CPE-8412073.

References

[1]Abramovich, G. N., *The Theory of Turbulent Jets*, MIT Press, Cambridge, MA, 1963.

[2]Harsha, P. T., "Free Turbulent Mixing: A Critical Evaluation of Theory and Experiment," Arnold Engineering Development Center, Tullahoma, TN, AEDC-TR-71-36, 1971.

[3]Durao, D., and Whitelaw, J. H., "Turbulent Mixing in the Developing Region of Coaxial Jets," *Journal of Fluids Engineering*, Sept. 1973, pp. 467-473.

[4]Antonia, R. A., and Bilger, R. W., "The Heated Round Jet in a Coflowing Stream," *AIAA Journal*, Vol. 14, No. 11, 1976, pp. 1541-1546.

[5]Shuen, J. S., Solomon, A. S. P., Zhang, Q. F., and Faeth, G. M., "A Theoretical and Experimental Study of Turbulent Particle-Laden Jets," NASA CR 168293, Nov. 1983.

[6]Green, H. G., and Whitelaw, J. H., "Velocity and Concentration Characteristics of the Near Field of Round Jets," Imperial College, London, FS/85/02, Feb. 1985.

[7]Pitts, W. M., "Effects of Global Density and Reynolds Number Variations on Mixing in Turbulent, Axisymmetric Jets," National Bureau of Standards, Rept. NBSIR 86-3340, March 1986.

[8]Mostafa, A. A., Mongia, H. C., McDonell, V. G., and Samuelsen, G. S., "Evolution of Particle-Laden Jet Flows: A Theoretical and Experimental Study," *AIAA Journal*, Vol. 27, No. 2, Feb. 1989, pp. 167-183.

[9]Gouldin, F. C., Johnston, S. C., Kollman, W., and Schefer, R. W., "Nonreacting Mixing Flows," *Progress Energy Combustion Science*, Vol. 12, Dec. 1986, pp. 270-304.

[10]Yule, A. J., "Large-Scale Structure in the Mixing Layer of a Round Jet," *Journal of Fluid Mechanics*, Vol. 89, 1978, pp. 413-432.

[11]Antonia, R. A., and Bilger, R. W., "An Experimental Investigation of an Axisymmetric Jet in a Co-Flowing Air Stream," *Journal of Fluid Mechanics*, Vol. 61, 1973, pp. 805-822.

[12]Michalke, A., "A Survey of Jet Instability Theory," *Progress in Aerospace Sciences*, Vol. 21, 1984, pp. 159-199.

[13]Crow, S. C., and Champagne, F. H., "Orderly Structure in Jet Turbulence," *Journal of Fluid Mechanics*, 1971, Vol. 48, pp. 547-591.

[14]Chen, L. D., and Roquemore, W. M., "Visualization of Jet Flames," *Combustion and Flame*, Vol. 66, March 1986, pp. 81-86.

[15]Roquemore, W. M., Goss, L. P., Lynn, W. F., Chen, L. D., and Chen, T. H., "The Dynamic Structure of Propane Jet Diffusion Flames," *AIAA 26th Aerospace Sciences Meeting*, Jan. 1988.

[16]Enotiadis, A. C., Gladnick, P. G., Samuelsen, G. S., and LaRue, J. C., "Statistical and Spectral Properties of a Freon Jet in a Coflowing Stream," Western States Section Meeting of the Combustion Institute, Maui, HI, Oct. 1987.

[17]Schefer, R. W., and Dibble, R. W., "Rayleigh Scattering Measurements of Mixture Fraction in a Turbulent Nonreacting Propane Jet," Sandia National Laboratories, Livermore, CA, SAND85-8837, Nov. 1986, p. 48.

[18]Brighton, J. A., and Jones, J. B., "Fully Developed Turbulent Flow in Annuli," *Journal of Basic Engineering*, Vol. 86, Dec. 1964, pp. 835-844.

[19]Laufer, J. "The Structure of Turbulence in Fully Developed Pipe Flow," NACA TN 2954, 1953.

[20]Corrsin, S., and Uberoi, M. S., "Further Experiments on the Flow and Heat Transfer in a Heated Turbulent Air Jet," NACA TN 1865, April 1949.

[21]Thring, M. W., and Newby, M. P., "Combustion Length of Enclosed Turbulent Jet Flames," *Fourth Symposium (International) on Combustion*, Combustion Institute, Pittsburgh, PA, 1953, pp. 789-796.

[22]Champagne, F. H., and Wygnanski, I. J., "An Experimental Investigation of Coaxial Turbulent Jets," *International Journal of Heat and Mass Transfer*, Pergamon, New York, Vol. 14, May 1971, pp. 1445-1464.

[23]Wygnanski, I. J., and Petersen, R. A., "Coherent Motion in Excited Free Shear Flows," *AIAA Journal*, Vol. 25, Feb. 1987, pp. 201-213.

[24]Gladnick, P. G., LaRue, J. C., and Samuelsen, G. S., "Velocity and Concentration Characteristics of a Turbulent Jet in a Coflowing Stream," Fourth International Symposium on Applications of Laser Anemometry of Fluid Mechanics, Lisbon, Portugal, July 1988.

[25]"Photomultipliers," Thorn-EMI Electron Tubes Ltd., Middlesex, England, PMC/86, 1986, pp. 1-21.